Characterization of the Low Temperature Superconductor Niobium Carbonitride

Mark J. Raine and Damian P. Hampshire

***Abstract*—Niobium carbonitride's superior radiation tolerance [1], coupled with the recently reported increase in its upper critical magnetic field when made nanocrystalline, increases its potential importance in future technological high-field superconductor applications. The maximum transition temperature for the composition $NbC_{0.3}N_{0.7}$ is ~17.8 K [2] and its upper critical magnetic field is ~11 T; this increases to ~12 T for the composition $NbC_{0.2}N_{0.8}$ [3], [4]. Using solid-state processing, we have fabricated microcrystalline bulk niobium carbonitride with a transition temperature of ~17.6 K. A comprehensive characterization of this material, which includes susceptibility, resistivity, magnetization, heat capacity and XRD measurements is provided. Comparisons between the heat-treated material and the same material subjected to hot isostatic pressing are made so that the values of the intrinsic fundamental properties can be identified and their sensitivities to different fabrication processes determined.**

***Index Terms*—Carbonitride, characterization, hot isostatic pressing, NbCN, niobium.**

I. Introduction

THE superconducting materials Nb-Ti and Nb_3Sn are the workhorses of high-field superconductor applications because of their excellent critical superconducting properties and the ease with which wires can be formed from them. It is known, however, that the transition temperatures (T_c) and the critical current densities (J_c) of the A15 compounds, of which Nb_3Sn is one, are markedly suppressed by irradiation. Superconductors of the cubic B1 structure are however, more resilient to such irradiation [1] and would be an alternative to A15's for fusion applications if it were not for their inferior high-field superconducting properties.

Niobium carbonitride $(NbC_{0.3}N_{0.7})$ is a low temperature Type II superconductor with a B1 crystal structure. We have recently produced a large increase in the upper critical magnetic field $(B_{c2}(0))$ of this material by making it nanocrystalline [5]–[7]. With further improvements we are hoping to reach or even surpass that of Nb_3Sn. If this improvement is realized then Nb-C-N might become an important technological high-field superconductor in its own right and a possible alternative to Nb_3Sn for fusion applications.

The highest T_c reported for $NbC_{0.3}N_{0.7}$ is ~17.8 K by Matthias *et al.* in 1953 [2]. They produced the material by forming a solid solution of NbN and NbC. A description of their heat-treatment was not offered. Pessall *et al.* [8] produced material with a similar transition temperature to Matthias's. Geballe *et al.* [9] produced material with a $T_c \sim 17.38$ K and Williams *et al.* achieved "near" 17.8 K results [4]. Dew-Hughes *et al.* [1] were provided with material from Storms, which had a transition temperature of 17.6 K.

In preparation for further work on improving $B_{c2}(0)$ in nanocrystalline material, we report here a comprehensive characterization of microcrystalline $NbC_{0.3}N_{0.7}$. The work provides a description of three samples that are representative of almost forty that have been fabricated. The intrinsic fundamental superconducting parameters are derived from a wide range of in-field measurements. These data provide an insight into the sensitivity of these parameters to the fabrication processes. Extrinsic properties such as J_c are also presented. We describe the different fabrication processes used to produce standard furnace heat-treated material and hot isostatically pressed material.

II. Fabrication, Hot Isostatic Pressing, and X-Ray Diffraction

A. Precursor Materials and Equipment

The precursor powders, NbC (product No. 12147) and NbN (product No. 12146), were both purchased from Alfa Aesar. A Carbolite three-zone 1800°C tube furnace (TZF 18/102/600) was used to heat-treat the samples. A bespoke, transportable sample-tube, which comprised of an internal and external alumina tube (EA998) sealed onto a stainless steel gas port assembly via a fluorocarbon compressed gasket, was used to provide a controlled nitrogen atmosphere for reacting the samples.

B. Preparation and Heat Treatment

The precursor binary materials were first hand-mixed in the correct proportions to produce the composition $NbC_{0.3}N_{0.7}$ prior to thorough mixing in a Fritsch planetary ball mill for 1 h at 200 rpm (direction reversed every 15 minutes) in a Nb vial without balls. The mixed powder was pressed into several 5 g pellets of approximate dimensions 11 mm diameter by 10 mm long. The pellets were then heat-treated at 1650°C (ramp rate $4.4°\mathrm{C/min}$) for 114 h prior to ramping the temperature down to 1360°C and dwelling for 4 h. Throughout the heat-treatment the samples were kept under flowing nitrogen. After the dwell period the furnace heaters were switched off and the furnace cooled at its natural rate. The long dwell time was used to improve homogeneity and the lower sintering temperature was used to control nitrogen content [4]. Three batches of pellets were produced in the furnace.

Although all pellets were touching each other and all within a distance of ~120 mm, we found that T_c varied within each batch; 17.5–17.7 K for batch $F1_{1650}$, sample $F2_{1650}$ was a batch

Manuscript received August 04, 2010; accepted November 13, 2010. Date of publication December 20, 2010; date of current version May 27, 2011. This work was supported by EPSRC.

The authors are with the Superconductivity Group, Durham University, Durham DH1 3LE, UK (e-mail m.j.raine@durham.ac.uk).

Digital Object Identifier 10.1109/TASC.2010.2095491

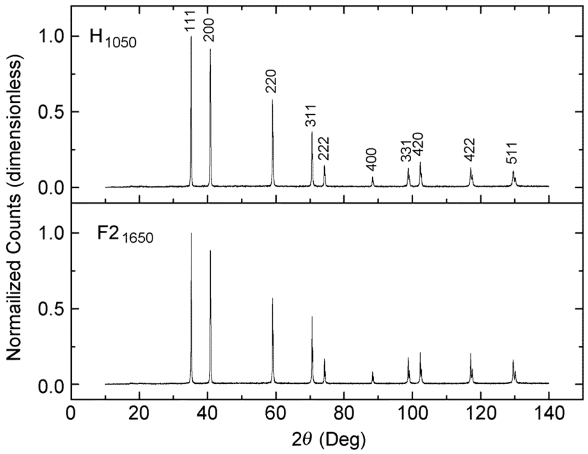

Fig. 1. X-Ray diffraction data of the heat-treated sample $F2_{1650}$ and the HIPed sample H_{1050}. Both data sets show single phase niobium carbonitride.

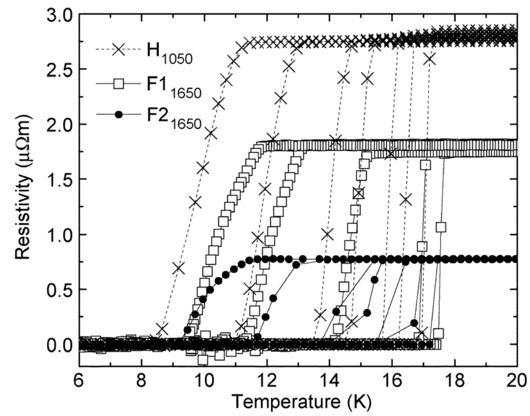

Fig. 2. Resistivity versus temperature for heat-treated and HIPed samples. Samples $F2_{1650}$ and H_{1050} were measured in fields 0, 0.5, 1.0, 2.0, 3.0, 5.5 and 8.0 T. Sample $F1_{1650}$ was measured in fields 0, 0.5, 3.0, 6.0 and 8.0 T.

of one pellet and 17.1–17.5 K for batch H_{1050}. Temperature profile measurements show that the temperature gradient across all of the pellets in any batch was negligible ($< 2^{\circ}C$). We suggest that low levels of oxygen contamination (not found in XRD data) were the probable source of the variation—consistent with the well-known affinity of Nb for oxygen. One sample was extracted from each of the first two batches—denoted $F1_{1650}$ and $F2_{1650}$.

C. Hot Isostatic Pressing (HIPing)

The third batch of pellets was powdered using a mortar and pestle. A HIP billet was formed by wrapping 3 g of powder in 0.025 mm thick niobium foil and then placing this packet into a 20 mm diameter stainless steel tube (316L), within an argon atmosphere. The stainless steel tube, which had one of its ends pre-welded, was attached to a vacuum pump whilst its unsealed end was sealed by flattening a section of it with a fly press and spot welding across the flat. The excess tube was removed and the spot welded join was then TIG welded to ensure the integrity of the enclosed vacuum. This enclosed sample was then put into the HIP and the pressure and temperature were both gradually raised to 2000 bar (in argon) and 1050°C in 1 h 22 min. A short dwell of approximately 10 minutes was maintained prior to reducing the pressure and temperature to ambient conditions in 1 h 30 min. The HIP'ed sample is denoted H_{1050}.

D. X-Ray Diffraction

X-Ray diffraction data were collected using a Siemens D500 diffractometer and were consistent with all three samples being single phase. Typical single-phase data are shown in Fig. 1 (for samples $F2_{1650}$ and H_{1050}). The splitting of the peaks at large detector angles is due to non-monochromatic radiation. We attribute small differences in peak heights to small differences in nitrogen content.

III. Results—Fundamental Properties

All measurements were made using a Quantum Design physical properties measurement system (PPMS).

TABLE I
Properties of $NBC_{0.3}N_{0.7}$. ρ_n: Normal State resistivity, T_c: Transition Temperature From Onset of Resistivity Data. δT_c: Transition Width (10%–90%) From Susceptibility Data, $J_c(B,T)$: Critical Current Density

Sample	ρ_n (μΩm)	T_c (K)	δT_c (K)	J_c(3T, 6K) (10^7 Am^{-2})	J_c(2T, 12K) (10^7 Am^{-2})
$F1_{1650}$	1.7	17.6	0.43	2.0	0.83
$F2_{1650}$	0.7	17.4	0.54	1.9	0.77
H_{1050}	2.7	17.2	0.48	0.8	0.28

A. Normal-State Resistivity, ρ_n

The resistivities of the furnace treated samples $F1_{1650}$ and $F2_{1650}$ and the HIP'ed sample H_{1050} were measured and are shown in Fig. 2 and normal state values are provided in Table I. The HIP'ed sample has the largest normal-state resistivity, which suggests poorer connections between grains compared to the furnace heat-treated samples, probably due to the relatively low temperature and short dwell-time of the HIP treatment. We also found that the resistivity of the furnace heat-treated sample $F1_{1650}$ was markedly different to $F2_{1650}$. We attribute these differences in resistivity to differences in the initial density of the pellets prior to furnace heat-treatment. The pellets were pressed by hand, with no means of ensuring a consistent pressure across batches. We suggest that in this refractory material, a lower initial density would alter the sintering dynamics, promoting coarsening over densification, and hence produce a sintered compact with inferior grain boundary contacts.

B. AC-Susceptibility

AC-Susceptibility in-field data for our three samples are shown in Fig. 3. Although all samples have similar (intrinsic) properties, sample $F1_{1650}$ has the highest T_c, characterized by the onset of the superconducting transition and a 10%–90% transition width of ~0.43 K (which is similar to that reported by Dew-Hughes [1]). The HIP'ed sample H_{1050} has the lowest T_c and the lowest $B_{c2}(T)$ values.

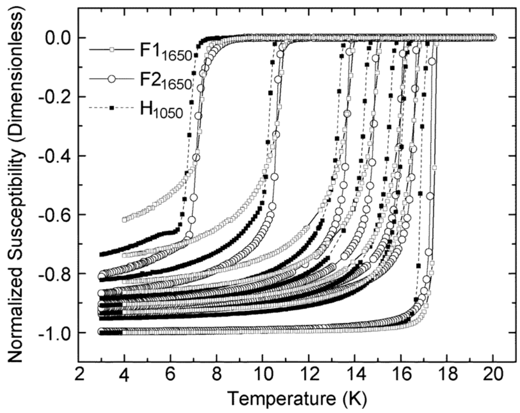

Fig. 3. Normalized susceptibility versus temperature for $F1_{1650}$, $F2_{1650}$ and H_{1050}, in applied fields of 0, 0.5, 1, 2, 3, 5.5 and 8 T. The data has been normalized by; $F1_{1650} - 2,08 \times 10^{-7}$, $F2_{1650} - 8.74 \times 10^{-7}$ and $H_{1650} - 5.51 \times 10^{-7}$ (Am^2) at low temperature and in zero-field.

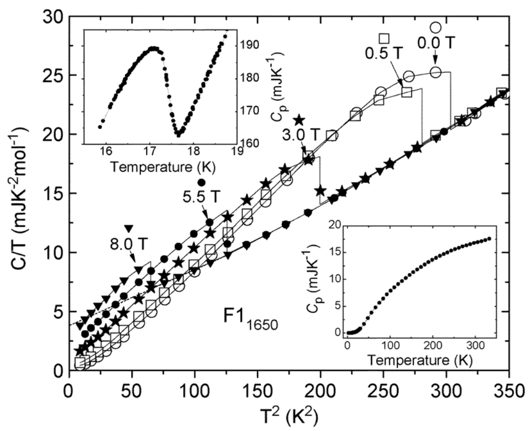

Fig. 4. Debye plot of sample $F1_{1650}$. The top inset shows the heat capacity at the superconducting transition in zero-field and the bottom inset shows the heat capacity from room temperature to 3 K. The thin line that intersects the y-axis is a linear extrapolation of the 8 T data at low temperatures in the normal-state and is used to determine the Sommerfeld constant.

C. Heat Capacity, C_p

Heat capacity data for sample $F1_{1650}$ were collected and are shown in Fig. 4 as a Debye plot following:

$$\frac{C}{T} = \gamma + \beta T^2 \tag{1}$$

$$\theta_D = \sqrt[3]{\frac{12}{5\beta}\pi^4 R} \tag{2}$$

where C is the heat capacity, γ (is the Sommerfeld constant, T is the temperature, β (is a constant that determines the Debye temperature θ_{D} (c.f. (2)) and R is the gas constant. A linear extrapolation of the low temperature normal-state 8 T data in Fig. 4 gives a value for γ (of 3.85 $\mathrm{mJ.K^{-2}mol^{-1}}$ and θ_{D} is 345 K. These values are similar to Geballe [9]; $\gamma = 3.26\ \mathrm{mJ.K^{-2}mol^{-1}}$ and $\theta_{\mathrm{D}} = 351$ K. Fig. 4 shows the expected suppression of the onset of superconductivity to lower temperatures with increasing applied fields.

D. Upper Critical Magnetic Field, $B_{c2}(T)$

The maximum $B_{c2}(0)$ reported for $\mathrm{NbC_{0.3}N_{0.7}}$ is ~11 T [3], [4]. Fig. 5 shows a compilation of our in-field data. $B_{c2}(T)$ versus temperature data are provided from ac-susceptibility, resistivity, magnetic hysteresis and heat capacity measurements on all three samples. The dashed curve in the figure represents the best-fit of (3) to all data points.

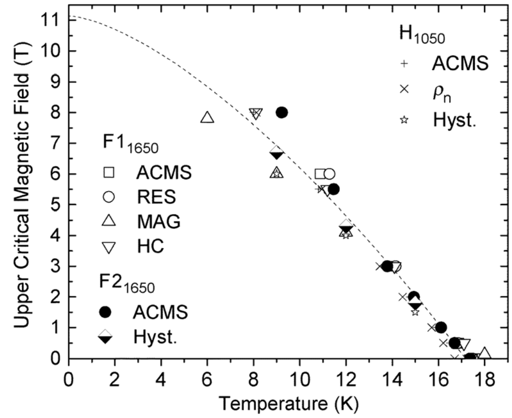

Fig. 5. Upper critical magnetic field versus temperature for samples $F1_{1650}$, $F2_{1650}$ and H_{1050}. The data are taken from ac-susceptibility, resistivity (ρ_{n}), magnetic hysteresis and heat capacity (C_{p}) measurements. The dashed line is a best-fit curve through all data points.

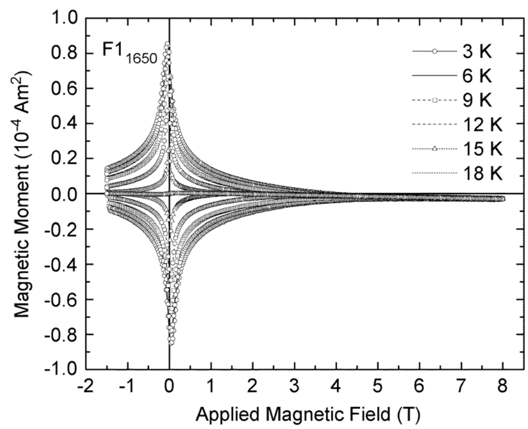

Fig. 6. Magnetic hysteresis data up to 8 T as a function of temperature for sample $F1_{1650}$.

$$B_{c2}(T) = B_{c2}(0)\left(1 - \left(\frac{T}{T_c}\right)^{\frac{3}{2}}\right) \tag{3}$$

The value of $B_{c2}(0)$ we have found is 11 ± 1.5 T.

IV. Results—Critical Current Density, J_C

Magnetic hysteresis data were collected for sample $F1_{1650}$ and are shown in Fig. 6. J_{c} of the sample was calculated using Bean's critical state model [10] for a superconducting slab (4)

$$J_c = \frac{\Delta m}{a_2\left(1 - \frac{a_2}{3a_1}\right)V} \tag{4}$$

where Δm is the change in the magnetic moment and a_1 and a_2 are the width and depth of the slab respectively, and V is the sample volume. Each of the measured samples was slab-like in shape and of millimeter dimensions—giving a typical uncertainty in J_{c} of ~10%. J_{c} as a function of applied field for sample $F1_{1650}$ is shown in Fig. 7(a) and that of sample H_{1050} is shown in Fig. 7(b). As shown in Table I, J_{c} of sample $F1_{1650}$ at 3 T and 6 K is ~ $2.0 \times 10^7\ \mathrm{Am^{-2}}$, which is low in comparison to the values reported for J_{c} in $\mathrm{Nb_3Sn}$ [11]. J_{c} of the HIPed sample H_{1050} is lower than that of sample $F1_{1650}$. The granularity of

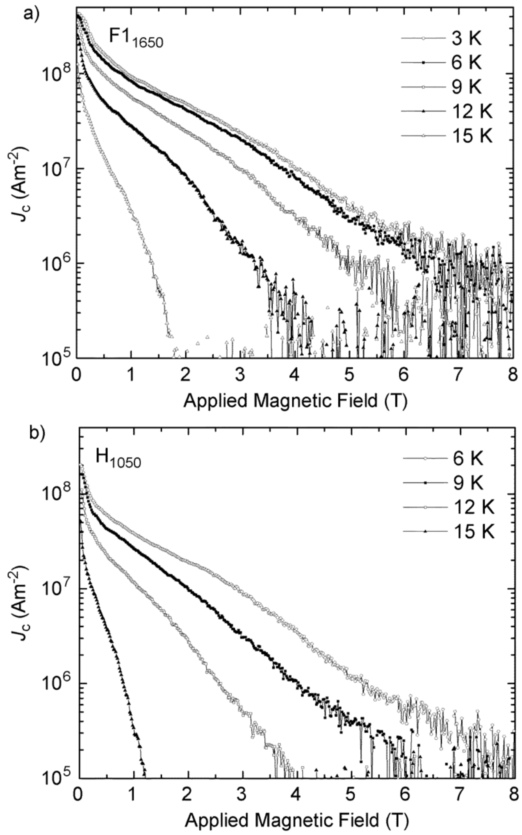

Fig. 7. Critical current density versus applied magnetic field (a) sample $\mathrm{F1}_{1650}$ and (b) sample H_{1050}.

this material has not, however, been optimized for high J_c and is to be the subject of future work.

V. Discussion

Standard terminology for superconducting materials usually describes as intrinsic, those properties characteristic of large ordered single crystals (e.g. T_c and B_{c2}). Extrinsic properties in contrast are predominantly determined by microstructure (e.g. J_c). Only when microstructural changes occur on the nanometer length-scale do we start to observe a complex interplay between intrinsic and extrinsic properties in high-field superconductors, because the microstructure is on the scale of the coherence length. For the three microcrystalline materials presented here, the grains are sufficiently large that as shown in Fig. 5, T_c and B_{c2} are similar, consistent with intrinsic properties. Equally the parameters derived from the heat capacity data, which is a volumetric measurement, are broadly unaffected by the grain boundaries and hence can also be considered intrinsic. In contrast the normal state values of resistivity vary by a factor of four between the samples. This can be attributed to the different processing procedures producing significantly different grain boundary properties. We interpret these results by suggesting that our samples consist of good intra-grain material separated by poorly connected grain boundaries. Consistent with this description, the HIP'ed sample H_{1050} had the highest resistivity and the lowest J_c. Given that its precursor was a ground, course-grained powder, which was probably insufficiently HIP'ed due to a short dwell time, it lends further support for such a description of our samples. Table II provides a list of the characterization parameters for $\mathrm{NbC_{0.3}N_{0.7}}$. The values of T_c and B_{c2} are broadly independent of the fabrication process in our samples. Equally γ and θ_D derived from $\mathrm{F1}_{1650}$ are consistent with the literature. We suggest that the first four parameters in Table II can be considered intrinsic. We also cite the lowest value of ρ_n we have found in our samples as an upper bound for the intrinsic resistivity. Finally, Table II provides the range of (extrinsic) J_c values we have observed.

TABLE II
Characterization Parameters for $\mathrm{NBC_{0.3}N_{0.7}}$. T_c: Transition Temperature. B_{c2}: Upper Critical Magnetic Field. J_c: Critical Current Density. ρ_n: Normal State Resistivity Just Above the Superconducting Transition. γ: Sommerfeld Constant. θ_D: Debye Temperature

Parameter	Values
T_c (K)	17.6 ± 0.5
$B_{c2}(0)$ (T)	11 ± 1.5
γ (mJK^{-2}mol^{-1})	3.85
θ_D (K)	345
ρ_n (μΩm)	< 0.7
J_c(B = 3 T) (Am^{-2})	0.8 - 2.0 x 10^7 (at 6 K)

VI. Conclusion

Samples have been fabricated which comprise of high-quality intra-grain material connected by poor grain boundaries. By considering a range of measurements made on a range of samples produced using different processing techniques, we have identified the intrinsic properties of $\mathrm{NbC_{0.3}N_{0.7}}$.

References

[1] D. Dew-Hughes and R. Jones, "The effect of neutron irradiation upon the superconducting critical temperature of some transition-metal carbides, nitrides, and carbonitrides," *Appl. Phys. Lett.*, vol. 36, p. 856, 1980.
[2] B. T. Matthias, "Transition temperature of superconductors," *Phys. Rev.*, vol. 92, p. 874, 1953.
[3] V. N. Troitskiy *et al.*, "Synthesis and characteristics of ultra-fine superconducting powders in the Nb-N, Nb-N-C, Nb-Ti-N-C systems," *J. Nanoparticle Res.*, vol. 5, p. 521, 2003.
[4] M. W. Williams, K. M. Ralls, and M. R. Pickus, "Superconductivity of cubic niobium carbo-nitrides," *J. Phys. Chem. Solids*, vol. 28, p. 333, 1967.
[5] H. J. Niu and D. P. Hampshire, "Disordered nanocrystalline superconducting $\mathrm{PbMo_6S_8}$ with a very large upper critical field," *Phys. Rev. Lett.*, vol. 91, p. 027002, 2003.
[6] D. M. J. Taylor, M. Al-Jawad, and D. P. Hampshire, "A new paradigm for fabricating bulk high-field superconductors," *Supercond. Sci. Tech*, vol. 21, p. 125006, 2008.
[7] M. J. Raine and D. P. Hampshire, Nanocrystalline $\mathrm{NbC_{0.3}N_{0.7}}$ With Very High Upper Critical Field unpublished.
[8] N. Pessall, C. K. Jones, H. A. Johansen, and J. K. Hulm, "Critical currents in niobium carbonitrides," *Appl. Phys. Lett.*, vol. 7, p. 38, 1965.
[9] T. Geballe and B. *et al.*, "High temperature SP-band superconductors," *Physics (New York)*, vol. 2, p. 293, 1966.
[10] C. P. Bean, "Magnetization of high-field superconductors," *Rev. Mod. Phys.*, vol. 36, p. 31, 1964.
[11] M. N. Wilson, *Superconducting Magnets*. Oxford: Oxford Univ. Press, 2002, p. 303.